6 Hodgkin and Huxley's Analysis of the Squid Giant Axon

6.1 Introduction

Electric signals in excitable cells are transmitted from one part of the cell to another in two ways: the passive spread of graded potentials and the propagation of all-or-none action potentials. Graded potentials are normally observed in interneurons that transmit signals over short distances, whereas action potentials are used by neurons that bear far-reaching processes (axons), carrying signals over long distances.

Graded potentials are carried by ions that diffuse down their electrochemical gradients, and the magnitude of the signal varies with the ionic currents. Action potentials, on the other hand, are carried by voltage- and time-dependent conductances that generate transient all-or-none potential changes (spikes or nerve impulses) that propagate from one part of the cell to another. The purpose of this chapter and part of the next chapter is to describe the basic mechanisms underlying the generation and propagation of action potentials. The best-studied preparation for action potentials is the squid giant axon, and the analytical tool is the gate model of Hodgkin and Huxley.

6.2 Voltage-clamp experiments of the squid axon

6.2.1 Voltage-clamp systems and reasons for voltage clamping

In order to analyze the nonlinear properties of ion conductances underlying action potentials, Hodgkin and Huxley performed a series of voltage-clamp experiments on the squid giant axon. Voltage-clamp experiments usually involve inserting two electrodes (in the case of the squid axon, two silver wires) into the axon, one for recording the transmembrane voltage

and the other for passing current into the axon to keep the transmembrane voltage constant (or clamped). The basic circuitry of the voltage-clamp experiment is shown in figure 6.1 and is discussed in appendix A.

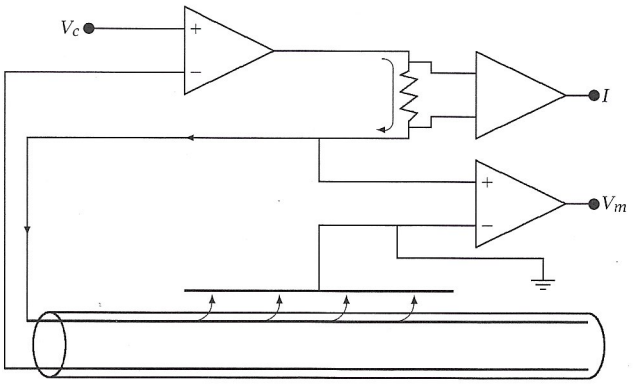

Figure 6.1 Schematic diagram of the two-wire voltage-clamp experiments on the squid axon. One wire is used for monitoring the membrane potential and the other for passing current. The voltage clamp amplifier injects or withdraws charges from the interior of the squid axon in order to hold the membrane voltage constant (voltage is clamped at the command voltage, V_c).

The reason for voltage-clamping the axon is threefold: (1) By keeping the voltage constant, one can eliminate the capacitive current, that is, $I_C = C\frac{dV}{dt} = 0$; (2) by keeping the voltage constant, one can measure the time-dependent characteristics of ion conductances without the influence of voltage-dependent parameters; and (3) by inserting two silver wire electrodes into the axon, one can space-clamp it so that the whole length of the axon is isopotential (silver wires short-circuit the interior of the axon).

6.2.2 Voltage-clamp records

Under voltage-clamp conditions, the current responses to voltage steps reflect the change of ion currents flowing across the membrane. Figure 6.2 shows the current records of the squid axon when the voltage is stepped from a holding voltage (V_H) to a command voltage (V_c) of various levels. When V_c is above -30 mV, a transient inward current followed by a sustained outward current is observed. The amplitude of the early inward current first increases and then decreases as V_c becomes more positive, whereas that of the late outward current increases monotonically with V_c.

So that the current record can be examined closely, current traces in response to $V_c = 0$ mV and $V_c = -120$ mV are given in the left part of figure 6.3. I_C is the capacitive current elicited by the transitions of volt-

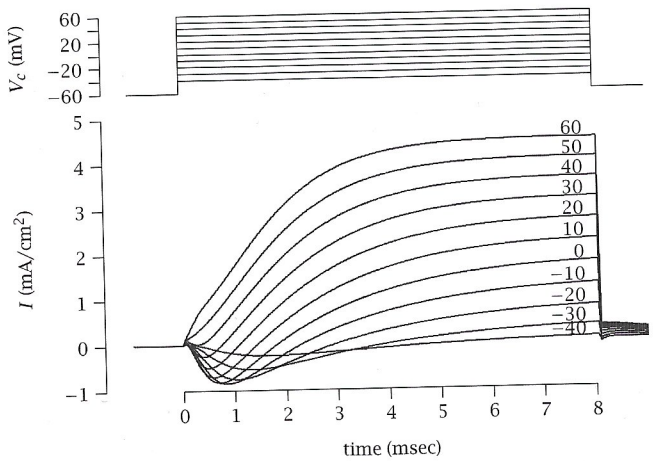

Figure 6.2 Currents measured with voltage clamp of squid axon. Membrane potential was held at −60 mV and then stepped (at 0 msec) to various potentials (shown at the right of each trace) for 8 msec before stepping back to −60 mV.

age from V_H to V_c. The membrane current consists of an early transient inward current and a late steady outward current. The I-V relations of the early and late currents are shown in the right part of figure 6.3.

It can be shown experimentally that the two currents are mediated by two separate conductances. If one removes extracellular Na^+ (which eliminates the driving force of the inward Na^+ flux) or adds tetrodotoxin (TTX, which blocks Na^+ channels), one can eliminate the early transient inward current mediated by Na^+ channels. On the other hand, if one removes intracellular K^+ or adds tetraethylammonium (TEA, which blocks K^+ channels), one can eliminate the late outward current mediated by K^+ channels. The separation of the two currents is illustrated in figure 6.4.

6.2.3 Instantaneous current-voltage relation

The voltage-clamp analysis of the squid axon discussed in the previous section shows that I_{Na} and I_K can be measured independently. The next step is to determine g_{Na} and g_K. How is $I_{Na}(I_K)$ related to $g_{Na}(g_K)$? Do they follow Ohm's law (i.e., $I_{Na} = g_{Na}(V - E_{Na})$)? In order to obtain answers to these questions, Hodgkin and Huxley performed the following experiments. Two voltage pulses were applied to the axon. V_1 activates the early (Na^+) current I_1 (• in figure 6.5). While the Na^+ conductance was turned on at $V_1 = -29$ mV, the potential was suddenly stepped to V_2, and the instantaneous current I_2 (∘ in figure 6.5) was recorded. By measuring

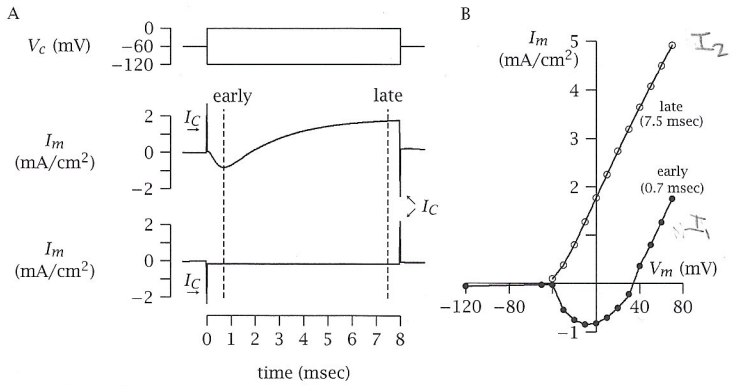

Figure 6.3 Early and late currents of a squid axon when the voltage is stepped from −60 mV to 0 mV or −120 mV (A); and the current-voltage relations of the early and late currents (B).

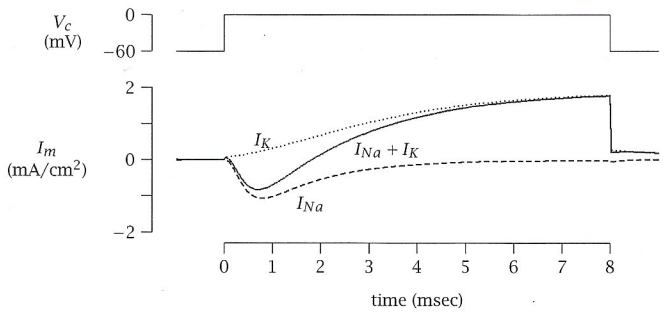

Figure 6.4 Separation of membrane current (solid trace) into Na^+ (dashed trace) and K^+ (dotted trace) currents. I_K is obtained in the presence of TTX or when $[Na^+]_{out} = 0$; I_{Na} is obtained in the presence of TEA. The voltage is stepped from −60 mV to 0 mV for 8 msec.

$I_2 - I_1$ as a function of $V_2 - V_1$, one can estimate the I-V relation of the Na^+ channels without time-dependent influence on the current.

For voltage pulse V_1, $I_{Na_1}(V_1, t_1) = g_{Na}(V_1, t_1)(V_1 - E_{Na})$. Then a sudden second voltage pulse V_2, $I_{Na_2}(V_2, t_1^*) = g_{Na}(V_2, t_1^*)(V_2 - E_{Na}) = g_{Na}(V_1, t_1)(V_2 - E_{Na})$ $(g_{Na}(V_1, t_1) = g_{Na}(V_2, t_1^*)$ because g_{Na} does *not* have enough time to change). Therefore, $I_2 - I_1 = g_{Na}(V_1, t_1)(V_2 - V_1)$. $g_{Na}(V_1, t_1)$ is a constant at a fixed voltage V_1 and fixed time t_1. Thus, Ohm's law predicts that $(I_2 - I_1)$ and $(V_2 - V_1)$ are linearly related. Experimental results, shown in figure 6.5, indicated that this is true for the squid axon. I_2 vs. V_2 is a straight line, which implies that $(I_2 - I_1)$ vs. $(V_2 - V_1)$ is a straight line because $I_1(V_1)$ and V_1 are constants. Note that I_1 and I_2 intersect at two points. The left intersecting point is obviously V_1, the

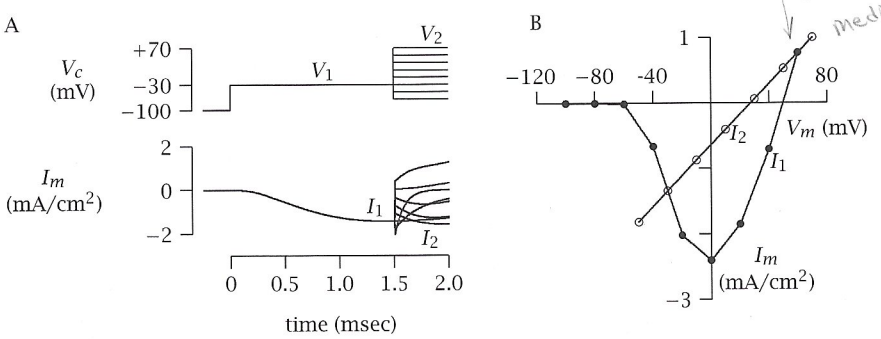

Figure 6.5 Instantaneous current-voltage relation (B) obtained with voltage clamp for the early inward channel (A). Closed circles indicate normal peak inward current for various depolarizations. Open circles indicate variation of I_2 with V_2 as shown in the intersection on right. $I_2 - I_1$, instantaneous step of current produced by voltage step $V_1 - V_2$. Duration of first pulse = 1.5 msec. (After Hodgkin and Huxley 1952b.)

first voltage pulse; the right intersecting point is E_{Na}, because $I_1(V) = g(V, t_1)(V - E_{Na})$ (• in figure 6.5), and $I_2(V, V_1, t_1^*) = g(V_1 t_1^*)(V - E_{Na})$(∘ in figure 6.5). $I_1(V) = I_2(V, V_1, t_1^*)$ only under two conditions: (1) $V = V_1$, thus $g(V, t_1) = g(V_1, t_1) = g(V_1, t_1^*)$ (left intersecting point); or (2) $V = E_{Na}$, thus $V - E_{Na} = 0$, therefore, $I_1(V) = I_2(V, V_1, t_1) = 0$ (right intersecting point).

The right intersecting point of I_1 and I_2 is E_{Na}, but it does not lie on the V-axis ($I = 0$). This indicates that I_1 is not totally mediated by Na^+, because if it were so, I_1 should be 0 when $V = E_{Na}$. The explanation for the nonzero I_1 at $V = E_{Na}$ is that at $t = t_1 = 1.53$ msec, I_K is nonzero although its value is far from the steady-state maximum level (8 msec). $I_1 (= I_{Na} + I_K)$ is therefore shifted toward more positive values in the I-V plot.

Similar experiments were performed for the late (K^+) channels, and the results are shown in figure 6.6. V_1 is about +20 mV (right intersecting point of I_1 and I_2), and E_K is about −80 mV (left intersecting point). The instantaneous K^+ current is also linear.

The above experiments show that $I_{Na}(I_K)$ and $g_{Na}(g_K)$ are related by Ohm's law in the squid axon. Thus by measuring I_{Na} and I_K experimentally, Hodgkin and Huxley were able to determine g_{Na} and g_K by simply dividing the currents by their driving forces, $(V - E_{Na})$ and $(V - E_K)$.

It is worth noting, however, that not all excitable cells exhibit linear instantaneous I-V relations for Na^+ and K^+ channels; for example, nodes of Ranvier do not.

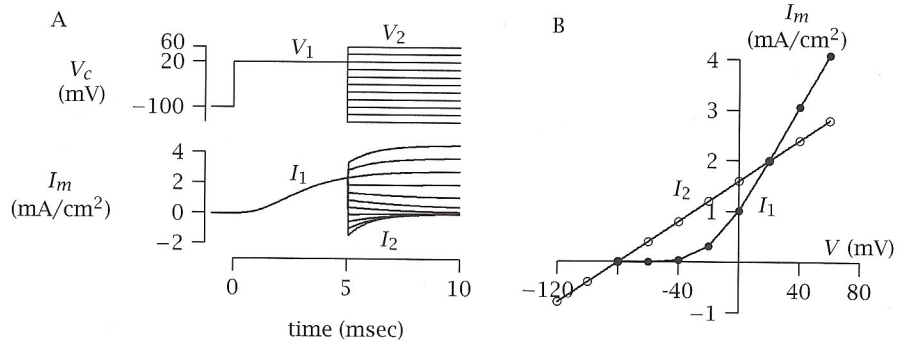

Figure 6.6 Instantaneous current-voltage relation obtained with voltage clamp for the late outward current. Similar protocols are used for the late current as for the early current (see figure 6.5).

6.2.4 g_{Na} and g_K of the squid axon

From the analysis described in the last section, it can be seen that the instantaneous Na^+ and K^+ conductances in the squid axon are linear. This allowed Hodgkin and Huxley to obtain $g_{Na}(V,t)$ and $g_K(V,t)$ by dividing $I_{Na}(V,t)$ and $I_K(V,t)$ (from their voltage-clamp data) by $(V - E_{Na})$ and $(V - E_K)$, respectively. The procedures and results are shown in figure 6.7.

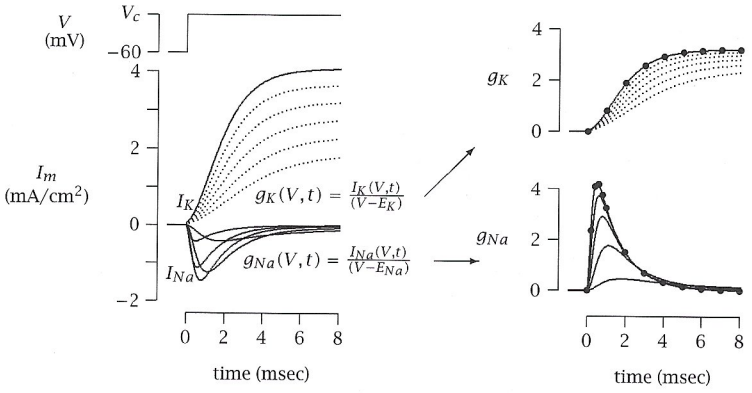

Figure 6.7 Time course of g_K (dashed traces) and g_{Na} (solid traces) at various voltages (V_c) obtained from I_K and I_{Na} traces, according to Ohm's law.

6.3 Hodgkin and Huxley's model

Using the experimental results of $g_{Na}(V,t)$ and $g_K(V,t)$ described in the previous section and the gate model in the last chapter, Hodgkin and Huxley proposed a landmark model that quantitatively described the behavior of Na^+ and K^+ channels, nerve excitation, and conduction. First, they used the parallel conductance model to describe the major ionic conductances in the squid axon.

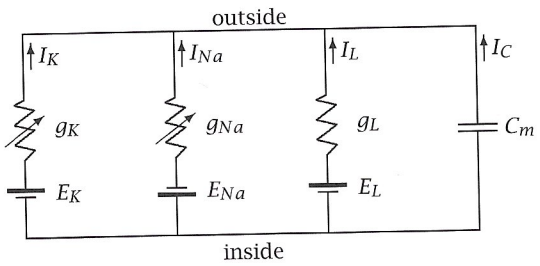

Figure 6.8 Parallel conductance model for the squid axon. g_K and g_{Na} are voltage and time dependent, and g_L is constant. The total membrane current is described by equation 6.3.1.

$$I_m = C_m \frac{dV}{dt} + I_K + I_{Na} + I_L,$$

where I_L = leak current, which is carried mainly by Cl^- and other ions, since all currents obey Ohm's law. Thus,

$$I_m = C_m \frac{dV}{dt} + g_K(V,t)(V - E_K) + g_{Na}(V,t)(V - E_{Na}) + g_L(V - E_L). \tag{6.3.1}$$

Hodgkin and Huxley proposed that the Na^+ and K^+ conductances were controlled by gating particles, and thus g_K and g_{Na} can be written as products of gating variables and maximum conductances:

$$g_K(V,t) = Y_K(V,t)\overline{g}_K,$$

and

$$g_{Na}(V,t) = Y_{Na}(V,t)\overline{g}_{Na},$$

where Y_K and Y_{Na} are gating variables between 0 and 1, and $\overline{g}_K$ and $\overline{g}_{Na}$ are maximum conductances.

From the time course of the *measured* g_{Na} and g_K (see the previous section), Hodgkin and Huxley found that Y_K and Y_{Na} do *not* follow simple exponentials (thus not a single $y(t)$; see gate model in chapter 5). Instead, they follow power functions of the exponential. Thus Hodgkin and Huxley proposed:

$$g_K(V,t) = Y_K(V,t)\overline{g}_K = n^4\overline{g}_K,$$

and

$$g_{Na}(V,t) = Y_{Na}(V,t)\overline{g}_{Na} = m^3h\overline{g}_{Na},$$

where n, m, and h are the gating variables ($y(t)$, see chapter 5) in the gate model and follow first-order kinetics (exponential time course). Recalling the kinetics of the gating variable $y(t)$, one can write $n(t)$, $m(t)$, and $h(t)$ the same way:

$$\frac{dn}{dt} = \alpha_n(1-n) - \beta_n n, \quad n_\infty = \frac{\alpha_n}{\alpha_n+\beta_n}, \quad \tau_n = \frac{1}{\alpha_n+\beta_n}. \tag{6.3.2}$$

$$\frac{dm}{dt} = \alpha_m(1-m) - \beta_m m, \quad m_\infty = \frac{\alpha_m}{\alpha_m+\beta_m}, \quad \tau_m = \frac{1}{\alpha_m+\beta_m}. \tag{6.3.3}$$

$$\frac{dh}{dt} = \alpha_h(1-h) - \beta_h h, \quad h_\infty = \frac{\alpha_h}{\alpha_h+\beta_h}, \quad \tau_h = \frac{1}{\alpha_h+\beta_h}. \tag{6.3.4}$$

Equations 6.3.2, 6.3.3, and 6.3.4 yield the following solutions: (see gate model in the last chapter for $y(t)$):

$$n(t) = n_0 - \left[(n_0 - n_\infty)\left(1 - e^{-t/\tau_n}\right)\right],$$

$$m(t) = m_0 - \left[(m_0 - m_\infty)\left(1 - e^{-t/\tau_m}\right)\right],$$

and

$$h(t) = h_0 - \left[(h_0 - h_\infty)\left(1 - e^{-t/\tau_h}\right)\right],$$

or

$$h(t) = h_\infty + \left[(h_0 - h_\infty)e^{-t/\tau_h}\right].$$

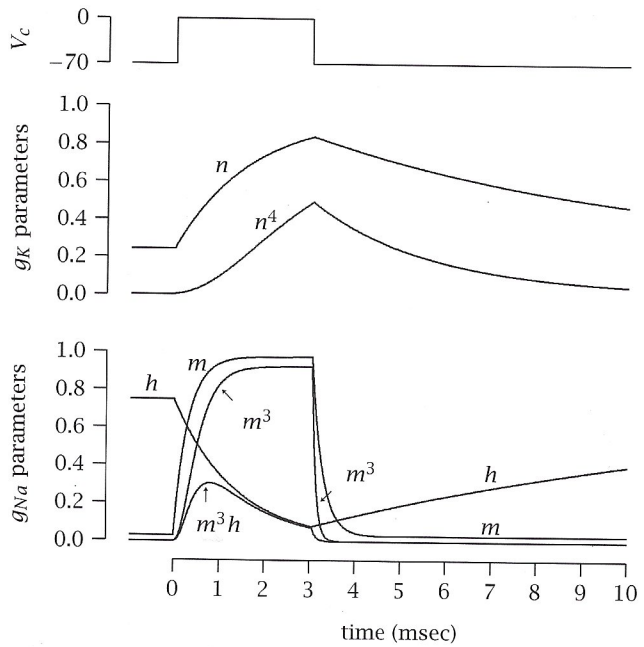

Figure 6.9 Time courses of n, n^4, m, m^3, h, and m^3h following a depolarizing voltage step (from −70 mV to 0 mV; duration of the step is 3 msec). n and m follow the $(1 - e^{-t/\tau})$ time course (activated by depolarization), whereas h follows the $e^{-t/\tau}$ time course (inactivated by depolarization).

Note that n and m are in $(1 - e^{-t/\tau})$ form and h is in the form $e^{-t/\tau}$ because of the difference in boundary conditions. That is, $h_0 > h_\infty$, whereas $n_\infty > n_0, m_\infty > m_0$. n and m are *activated by depolarization,* whereas h is *inactivated by depolarization.* One can then substitute the solutions of $n(t)$, $m(t)$, and $h(t)$ into $g_K(t)$ and $g_{Na}(t)$:

$$g_K(t) = \overline{g}_K n^4 = \overline{g}_K \left[n_0 - (n_0 - n_\infty)(1 - e^{-t/\tau_n}) \right]^4. \tag{6.3.5}$$

$$\begin{aligned} g_{Na}(t) &= \overline{g}_{Na} m^3 h \\ &= \overline{g}_{Na} \left[m_0 - (m_0 - m_\infty)(1 - e^{-t/\tau_m}) \right]^3 \left[h_\infty + (h_0 - h_\infty) e^{-t/\tau_h} \right] \\ &= \overline{g}_{Na} m_\infty^3 h_0 \left(1 - e^{-t/\tau_m}\right)^3 e^{-t/\tau_h}, \end{aligned} \tag{6.3.6}$$

because m_0 and h_∞ are neglectably small. The time course of g_K and g_{Na} described by equations 6.3.5 and 6.3.6 fitted the experimental data very well (see figure 6.7; smooth lines are equations 6.3.5 and 6.3.6, and circles are data points). The gate model also provides a quantitative description of the voltage dependence of g_K and g_{Na} as follows.

$$\alpha_n(V) = \alpha_n^0 e^{\gamma zFV/RT} \qquad n_\infty(V) = \frac{\alpha_n(V)}{\alpha_n(V)+\beta_n(V)}$$
$$\beta_n(V) = \beta_n^0 e^{-(1-\gamma)zFV/RT} \qquad \tau_n = \frac{1}{\alpha_n(V)+\beta_n(V)}$$

$$\alpha_m(V) = \alpha_m^0 e^{\gamma zFV/RT} \qquad m_\infty(V) = \frac{\alpha_m(V)}{\alpha_m(V)+\beta_m(V)}$$
$$\beta_m(V) = \beta_m^0 e^{-(1-\gamma)zFV/RT} \qquad \tau_m = \frac{1}{\alpha_m(V)+\beta_m(V)}$$

$$\alpha_h(V) = \alpha_h^0 e^{-(1-\gamma)zFV/RT} \qquad h_\infty(V) = \frac{\alpha_h(V)}{\alpha_h(V)+\beta_h(V)}$$
$$\beta_h(V) = \beta_h^0 e^{\gamma zFV/RT} \qquad \tau_h = \frac{1}{\alpha_h(V)+\beta_h(V)}$$

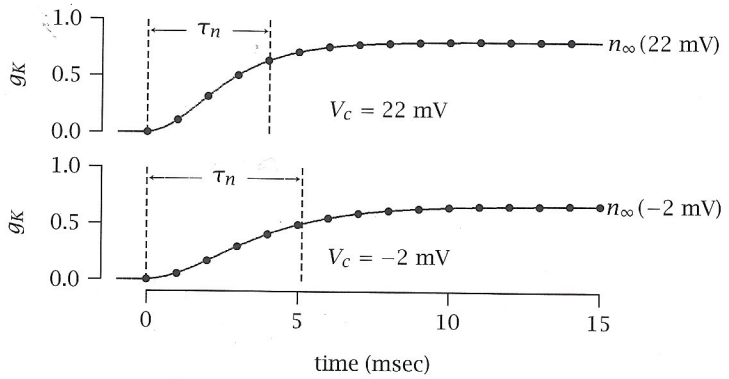

Figure 6.10 Measurement of τ_n and n_∞ from g_K traces at two voltages (−2 mV and 22 mV).

Hodgkin and Huxley determined all of the above parameters from their experimental data in the following way. They first measured τ_n, τ_m, τ_h, n_∞, m_∞, and h_∞ from the time records of g_K and g_{Na} at various voltages (an example is given in figure 6.10 for measuring τ_n and n_∞ at two voltage levels), and then they calculated α_n, β_n, α_m, β_m, α_h, and β_h by the following relationships:

$$\alpha_n = n_\infty/\tau_n \qquad \beta_n = (1 - n_\infty/\tau_n),$$
$$\alpha_m = m_\infty/\tau_m \qquad \beta_m = (1 - m_\infty)/\tau_m,$$
$$\alpha_h = h_\infty/\tau_h \qquad \beta_h = (1 - h_\infty)/\tau_h.$$

Hodgkin and Huxley plotted the values of α and β against transmembrane voltage and found that they can be fitted by the following empirical equations:

$$\alpha_n(V) = 0.01(-V + 10)/\left[e^{\frac{-V+10}{10}} - 1\right], \tag{6.3.7}$$

$$\beta_n(V) = 0.125e^{\frac{-V}{80}}, \tag{6.3.8}$$

$$\alpha_m(V) = 0.1(-V+25)/\left(e^{\frac{-V+25}{10}} - 1\right), \tag{6.3.9}$$

$$\beta_m(V) = 4e^{\frac{-V}{18}}, \tag{6.3.10}$$

$$\alpha_h(V) = 0.07e^{\frac{-V}{20}}, \tag{6.3.11}$$

$$\beta_h(V) = 1/\left(e^{\frac{-V+30}{10}} + 1\right). \tag{6.3.12}$$

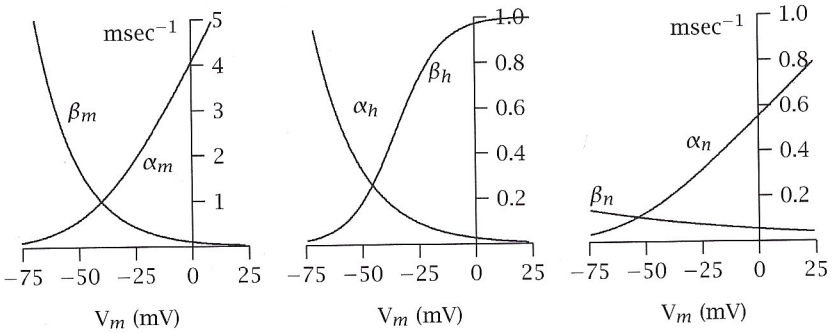

Figure 6.11 Voltage dependence of the rate coefficients of the Hodgkin and Huxley model.

These plots are shown in figure 6.11. It is important to note that the α's and β's in figure 6.11 follow the function $\alpha(V)$ and $\beta(V)$ predicted by the gate model (figures 5.9 and 5.10). α_n and α_m increase with membrane depolarization because n and m particles are activated by membrane depolarization. α_h decreases with membrane depolarization because the h particle is inactivated by depolarization.

Using the equations given above, the values of n_∞, m_∞, h_∞, τ_n, τ_m, and τ_h are calculated and plotted in figure 6.12. The m_∞, h_∞, and n_∞ also follow the y_∞ function predicted by the gate model (figures 5.9 and 5.10). The $n_\infty(V)$, m_∞, and h_∞ are called the steady-state *activation curves.* They give the voltage range and slope of activation for voltage-gated channels.

Equations 6.3.2–6.3.12, shown in the last section, are called the Hodgkin and Huxley equations. By putting them in equation 6.3.1, one obtains

$$I_m = C_m\frac{dV}{dt} + \overline{g}_K n^4(V - E_K) + \overline{g}_{Na} m^3 h(V - E_{Na}) + g_L(V - E_L).$$

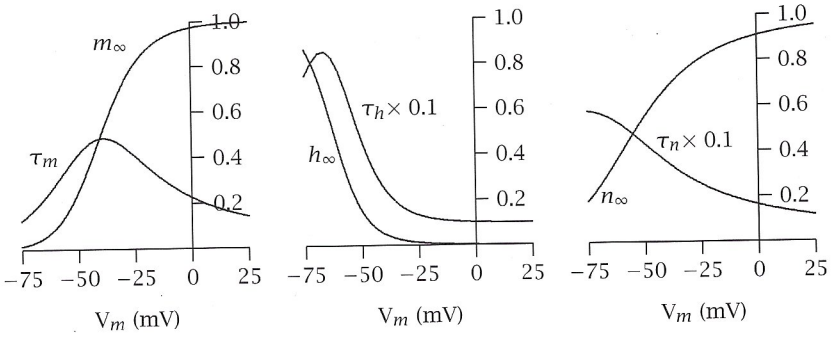

Figure 6.12 Steady-state activation curves (n_∞, m_∞, and h_∞) and the voltage dependence of the time constants of the Hodgkin and Huxley model.

Using numerical methods, Hodgkin and Huxley solved these equations and obtained remarkable fits between the recorded and the calculated action potentials (figure 6.13, left). Moreover, the calculated voltage-clamp records (figure 6.13, right) fit the experimental data very well.

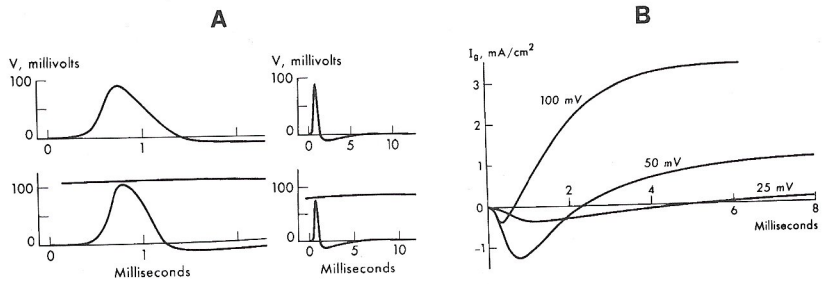

Figure 6.13 (A) Calculations, above, and experimental records, below, for propagating impulse on fast time scale, left, and slow scale, right; and (B) the ionic membrane currents after the indicated potential increase as calculated from the Hodgkin-Huxley equations. (From Cole 1968.)

Hodgkin and Huxley's model is certainly a triumph of classical biophysics in answering fundamental biological questions. Not only does it give quantitative accounts of Na^+ and K^+ fluxes, voltage- and time-dependent conductance changes, and the waveforms of action potentials, but also, as we will see next, it accounts for the conduction of action potentials along nerve fibers.

6.4 Nonpropagating and propagating action potentials

6.4.1 Hodgkin and Huxley equations for nonpropagating and propagating action potentials

For cells that are space-clamped and for which the membrane can be excited uniformly, cable properties are not involved, and the action potential is *nonpropagating:*

$$I_m = C_m \frac{dV}{dt} + I_K + I_{Na} + I_L \quad \text{(nonpropagating)}.$$

However, under physiological conditions, neurons are not voltage- or space-clamped, and action potentials initiated at one point will propagate along the axon. To describe action potential propagation, one should first derive the cable equation that illustrates how ions diffuse along the axons.

The equivalent circuit of a cable is given in figure 6.14 (see also chapter 4). V_m is now a function of time *and* distance.

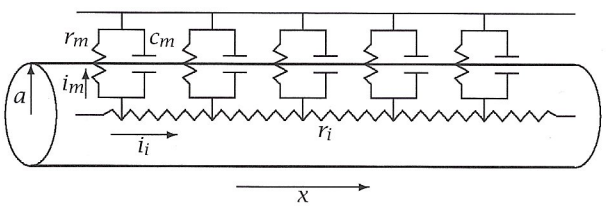

Figure 6.14 Schematic diagram illustrating current flow along a cylindrical axon (see figure 4.7).

Along the x-axis, $$\frac{\partial V_m(x,t)}{\partial x} = -r_i i_i. \tag{6.4.13}$$

Some of i_i, however, leaks out across the membrane through r_m and c_m, so i_i is not constant with distance.

$$\frac{\partial i_i}{\partial x} = -i_m. \tag{6.4.14}$$

Combining equations 6.4.13 and 6.4.14,

$$\frac{\partial^2 V_m}{\partial x^2} = -r_i \frac{\partial i_i}{\partial x} = r_i i_m.$$

Thus,

$$i_m = \frac{1}{r_i}\frac{\partial^2 V_m}{\partial x^2}. \tag{6.4.15}$$

From linear cable theory (chapter 4), the membrane current I_m along a cable is given by

$$I_m = \frac{a}{2R_i}\frac{\partial^2 V}{\partial x^2}.$$

Combining equation 6.4.1 with the equation for current in the parallel conductance model, we have

$$I_m = \frac{a}{2R_i}\frac{\partial^2 V}{\partial x^2} = C_m\frac{\partial V}{\partial t} + I_K + I_{Na} + I_L.$$

This is a second-order partial differential equation, which is very difficult to solve. It is known, however, that action potentials propagate with a constant speed (at least in axons with constant diameter), so one can use the wave equation

$$\frac{\partial^2 V}{\partial x^2} = \frac{1}{\theta^2}\frac{\partial^2 V}{\partial t^2},$$

where θ = conduction velocity (cm/sec). This would simplify the propagating Hodgkin and Huxley equation to

$$\frac{a}{2R_i\theta^2}\frac{d^2 V}{dt^2} = C_m\frac{dV}{dt} + I_K + I_{Na} + I_L.$$

This is a second-order ordinary differential equation, which is relatively easy to solve. From this wave equation, one can obtain

$$\theta = \sqrt{Ka/2R_iC_m} \propto \sqrt{a}.$$

K is a constant which is experimentally estimated to be 10.47 (msec^{-1}). Hodgkin and Huxley calculated conduction velocity and obtained

$$\theta = \sqrt{Ka/2R_iC_m} = 18.8 \text{ m/sec},$$

while the experimentally measured value of conduction velocity in the squid axon is

$$\theta = 21.2 \text{ m/sec}.$$

The Hodgkin and Huxley equations therefore give a very good fit to the experimental data.

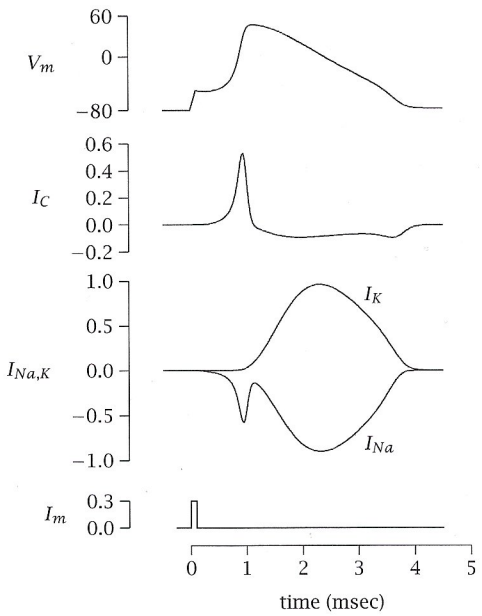

Figure 6.15 Voltage and current responses calculated for a nonpropagating action potential initiated by a brief square pulse current. The top diagram shows the potential change as a function of time. The second diagram shows the capacity current, I_C, given by $C_m dV/dt$. The initial, nearly square, wave is attributable to the applied current. The third diagram shows the K^+ and Na^+ components of the ionic current. Note that $I_m = I_C + I_K + I_{Na}$. (After Jack et al. 1975.)

6.4.2 Variations in voltage and currents during nonpropagating and propagating action potentials

Under certain conditions, the membrane of a cell or a portion of a cell can be excited uniformly and the cable complications can be eliminated. This can be achieved experimentally by space-clamping the cell (e.g., by inserting a long metal wire along the axon) or in cases where the cell is short enough for the membrane to be uniformly polarized during the action potential. In such circumstances, the relation between ion current flow across the membrane and the membrane potential is quite simple: All ionic current (I_i) is used to charge the local membrane capacitor, and none flows as local circuit (cable) current (figure 6.15). I_m is the stimulus current that initiated the action potential by depolarizing the cell above the threshold. I_m is zero during the action potential, thus

$$I_m = I_C + I_i = C_m \frac{dV}{dt} + I_i = 0; \text{ hence}$$

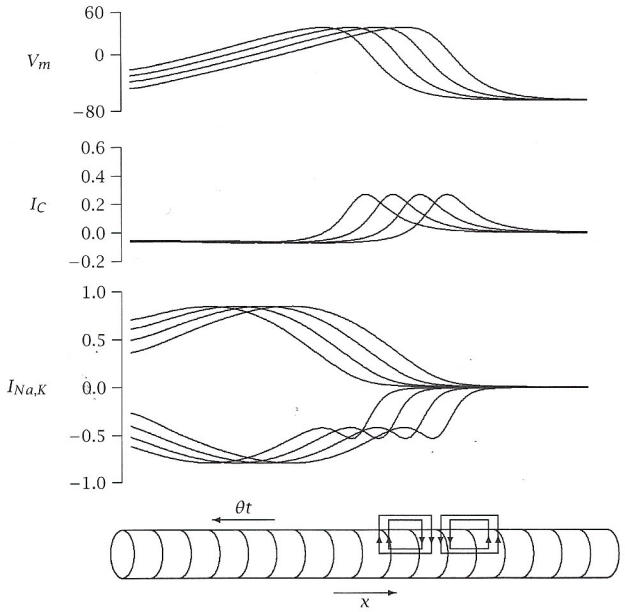

Figure 6.16 Calculated voltage changes and currents during an action potential propagated along an axon. The traces in each family of curves are separated by 0.1 msec. The top curve shows the membrane potential. Below are shown the changes in I_C, I_K and I_{Na}. The wave is propagating from right to left and, as noted in the text, the abscissa may also be regarded as time since $x = \theta t$. (After Jack et al. 1975.)

$$I_i = -I_C = -C_m \frac{dV}{dt} \text{ for nonpropagating action potentials.}$$

In the case of propagating action potentials, cable properties have to be considered. Figure 6.16 shows that an action potential is conducting from right to left. Upon arrival, the action potential depolarizes the local membrane, which causes an increase of g_{Na} and results in a net inward ionic current. This current enters the cell and diffuses laterally forward (left) and backward (right) along the axon and forms local circuit loops. The forward current depolarizes the local membrane and causes an increase of g_{Na}, which results in more inward current at that location. This process continues, causing the action potential to propagate in the forward direction. The backward current also depolarizes the local membrane, but since the action potential has just passed that location, the threshold is high (g_{Na} is low and g_K is high), and the action potential is not generated. The ionic current I_i in the propagating action potential not only charges the local membrane capacitor but also flows longitudinally and results in conduction of the action potential from one part of a cell to another.

6.5 Noble's model for nerve excitation: simplified I-V relations

In order to illustrate the characteristics of nerve and muscle excitation without going into too much mathematical detail, Noble (1966) made simplifying assumptions and provided a semiquantitative account of excitable membrane. This model is extremely useful for an intuitive understanding of membrane excitation. Assumptions: (1) m is significantly faster than n and h, so m will reach its steady-state value *almost* instantaneously at each potential. Since it is not, strictly speaking, instantaneous, we call it the *momentary I-V relation* for I_{Na}. (2) The instantaneous K^+ I-V relation is linear, as shown in squid axon (but not necessarily true in other cells). The momentary I-V relation of excitable membrane can be written as $I_i = I_{Na} + I_K$, which can be plotted as in figure 6.17.

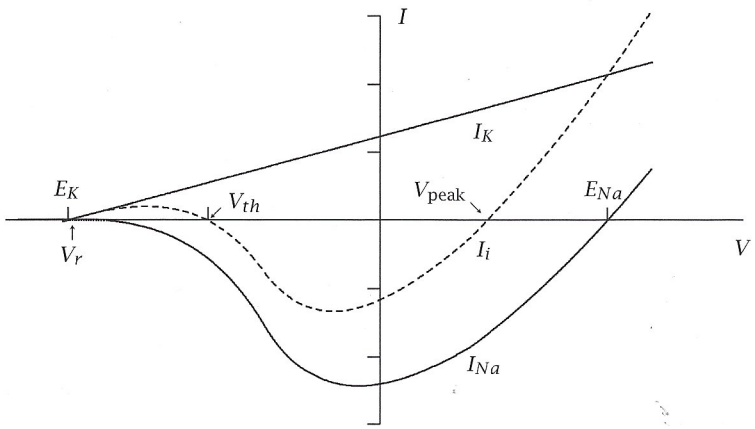

Figure 6.17 Diagram illustrating the form of simplified (momentary) current-voltage relation, $I_i = I_{Na} + I_K$, obtained by allowing fast Na^+ activation reaction (m) to be in a steady state while slower reactions (h and n) are held constant.

When the squid axon is at rest, the membrane is permeable primarily to K^+; thus the resting potential V_r ($I = 0$, the leftmost intersecting point) is very close to E_K. The slope conductance at this intersecting point is positive. This positive slope conductance makes V_r a *stable* point, because if a positive perturbation in V_m occurs, the I-V relation gives rise to an increment of positive (outward) current, which hyperpolarizes the cell and brings V_m back to V_r. For a negative V_m perturbation, the I-V relation gives rise to a negative (inward) current, which depolarizes the cell and brings V_m back to V_r.

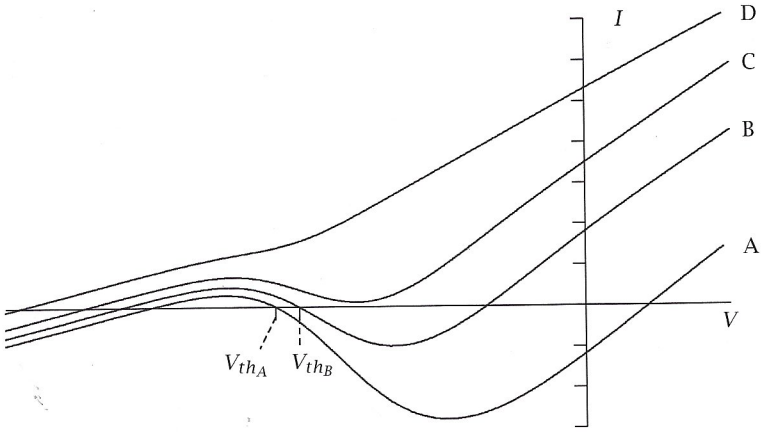

Figure 6.18 Diagram illustrating changes in momentary current-voltage relations with time on depolarization.

When the membrane potential reaches threshold V_{th} ($I = 0$, the middle intersecting point), the slope conductance is negative. This makes the I-V relation *unstable* because positive voltage perturbation results in negative (inward) current, which further depolarizes the cell and brings the potential further away from V_{th}. Negative voltage perturbation results in positive (outward) current, which further hyperpolarizes the cell. Therefore, when the membrane potential reaches V_{th}, it either depolarizes to generate an action potential, or hyperpolarizes back to V_r. Membrane potential never stably stays at V_{th}.

The rightmost intersecting point V_{peak} is the peak potential level an action potential can reach (when $g_{Na} >> g_K$). The slope conductance at this point is positive, and therefore the voltage should be stable in principle. However, the stability at V_{peak} is only transient because depolarization activates n and h, which increases I_K and decreases I_{Na}. This results in an outward shift of the I-V relation, and the time course of this shift is shown in figure 6.18 (A → B → C → D). Consequently, V_{peak} will become more negative and eventually disappear (when $I_K > I_{Na}$ at all potentials; C and D). Action potentials cannot be generated at instances C and D, and the membrane potential will spontaneously repolarize back to V_r.

By using these simplified I-V relations, one can explain the following important characteristics of actions potentials:

Threshold: Depolarizing current is needed to bring the membrane from a positive slope conductance region (E_r) to a negative slope conductance region for regenerative membrane potential change (dep → I_{inward} → dep

$\rightarrow I_{\text{inward}} \ldots$), which sets off the all-or-none action potential. Depolarization below threshold will result in repolarization back to V_r.

Accommodation: (Slow stimulus current is less effective than a rapid rising current to elicit excitation, and if the current is slow enough, excitation may not occur at all.) When the membrane is depolarized rapidly, the I-V relation will follow curve A because n and h do not have time to change appreciably, and thus the threshold will be at V_{th_A}. If the depolarization occurs slowly, then curve B will be followed because n increases and h falls, and the threshold will be at V_{th_B}, a higher value. If the depolarization occurs even more slowly, the I-V relation will follow curve C and there will be no threshold, and excitation will not occur. *Anode break* (an action potential observed at the offset of a hyperpolarizing current step) can be explained similarly.

Refractory period: During the action potential, the system moves from A to C and D, so that at the end of the action potential, the membrane is inexcitable (this is the absolute refractory period). After the action potential, the system moves back to B (relative refractory period—threshold high; V_{th} is more positive) and then to A (normal excitability).

6.6 Gating current

Hodgkin and Huxley (1952d) pointed out in their gate model that every voltage-dependent step must have an associated charge movement. Take the Na^+ channel as an example. Hodgkin and Huxley assumed that the Na^+ conductance is proportional to the probability of some gating particles that are near the *outside* of the membrane, that is,

$$g_{Na} = \overline{g}_{Na} y_{\text{out}}, \tag{6.6.16}$$

where

$$y_{\text{in}} + y_{\text{out}} = 1. \tag{6.6.17}$$

The gating particle can be in either of the two positions:
y_{in} = probability of gating particle on the inside, and
y_{out} = probability of gating particle on the outside.

Assuming the gating particles move *independently* in the membrane, then the probabilities of their being at any given state are proportional to $e^{-\xi/kT}$ where ξ is the energy of the particle in the state (Boltzmann's distribution). Thus,

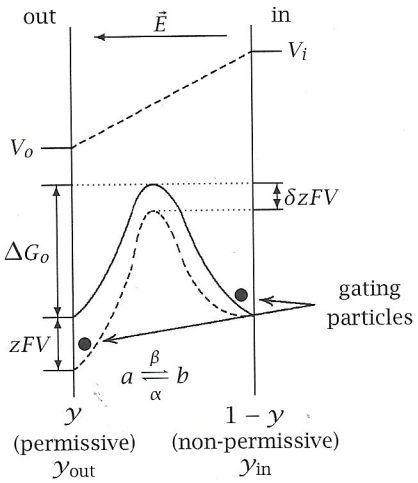

Figure 6.19 Energy profiles of a gating particle in the membrane under the influence of the electric field. y_{out} is the probability of the particle near the outside margin of the membrane and y_{in} is the probability of the particle near the inside margin. (See also legend for figure 5.9.)

$$y_{in} \propto e^{-\xi_{in}/kT}, \quad y_{out} \propto e^{-\xi_{out}/kT},$$

when a transmembrane voltage (V) is developed (see figure 6.19).

$$y_{in} \propto e^{-\xi_{in}/kT} \qquad y_{out} \propto e^{-(\xi_{out}-zeV)/kT}.$$

Therefore,

$$\frac{y_{out}}{y_{in}} = e^{-(\xi_{out}-\xi_{in})/kT+zeV/kT} = e^{(w+zeV)/kT},$$

where $w = -(\xi_{out} - \xi_{in})$ and is the work required for a particle to move across the membrane when $V = 0$, z = number of charges on the gating particle, e = elementary electric charge, V = membrane potential, k = Boltzmann's constant, and T = absolute temperature.

Combining equations 6.6.16 and 6.6.17, we get

$$g_{Na} = \overline{g}_{Na} \frac{e^{(w+zeV)/kT}}{1 - e^{(w+zeV)/kT}}. \tag{6.6.18}$$

When V is large and negative, $w << zeV$ and $e^{(w+zeV)/kT} << 1$.

$$g_{Na} \cong \overline{g}_{Na} e^{zeV/kT} = \overline{g}_{Na} e^{zV/25(\text{mV})}. \tag{6.6.19}$$

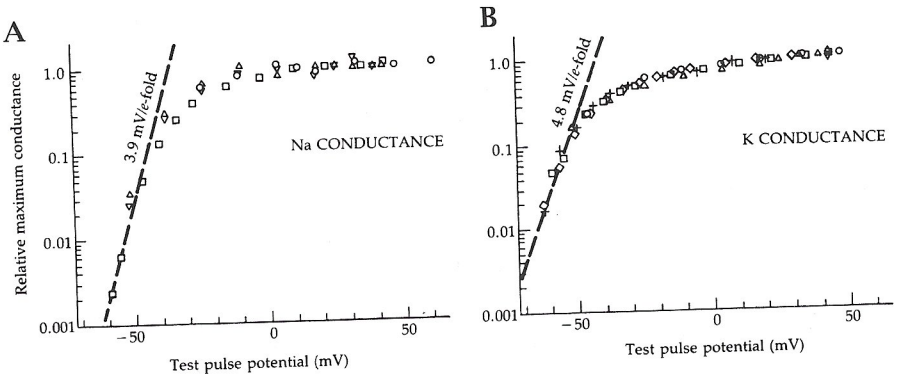

Figure 6.20 Peak g_{Na} (A) and steady-state g_K (B) are measured during depolarizing voltage steps under voltage clamp. Symbols are measurements from several squid giant axons, normalized to 1.0 at large depolarizations, and plotted on a logarithmic scale against the potential of the test pulse. Dashed lines show limiting equivalent voltage sensitivities of 3.9 mV per *e*-fold increase of g_{Na} and 4.8 mV per *e*-fold increase of g_K for small depolarizations. (From Hille 1992, adapted from Hodgkin and Huxley 1952a.)

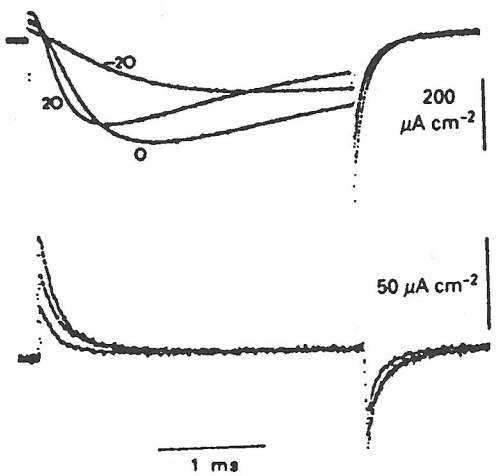

Figure 6.21 Na^+ ionic and gating currents in squid axon, produced during depolarizations under voltage clamp. The upper traces show currents recorded in an artificial sea water with only one fifth of the normal Na^+ concentration, for depolarizations from −70 mV to −20, 0, and +20 mV. The initial brief outward current is gating current, followed by the much larger inward Na^+ ionic current. The lower set shows the gating currents alone, after blockage of the Na^+ ionic currents with TTX. K^+ currents were eliminated by using K^+-free solutions for both internal and external media. (From Aidley 1989, adapted from Bezanilla 1986.)

Experimentally, Hodgkin and Huxley showed that for large negative potentials, $g_{Na} << \overline{g}_{Na}$ (figure 6.20A), and the semi-log plot shows that g_{Na} increases by e-fold for every 4 mV (3.9 mV) increase in membrane voltage.

Thus,

$$g_{Na} \propto e^{V/4(mV)}. \tag{6.6.20}$$

Comparing equations 6.6.19 and 6.6.20 yields that $z = 6$. Therefore, in order to open one Na^+ channel, 6 charges must move across the membrane or 3 dipoles must be reversed.

The movement of this gating charge is *outward* for *depolarizing* voltage pulse, and it gives rise to a small *outward current.* However, this outward *gating current* is masked by the inward Na^+ current and the outward capacitive current. In order to remove these currents, Armstrong and Bezanilla (1974) used Na^+-free solutions + TTX (blocks Na^+ channels) + Cs^+ internally to block K^+ channels. In addition, to eliminate the linear capacitive current, they averaged the responses to an equal number of positive and negative steps of potential from a negative holding level. The resultant average current is shown in figures 6.21 and 6.22A.

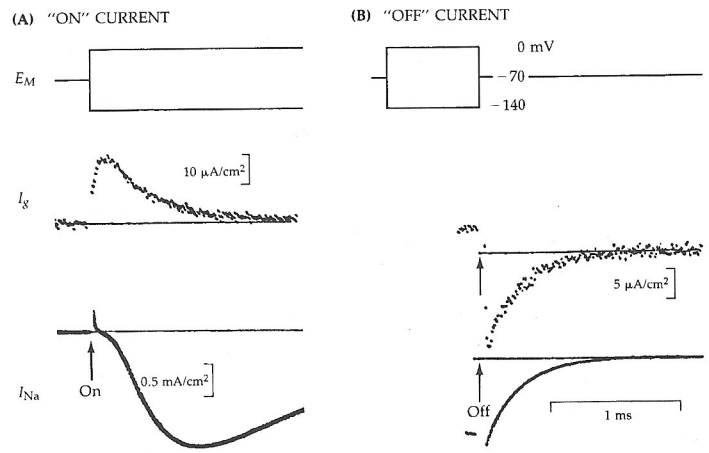

Figure 6.22 Gating current (I_g) and I_{Na} recorded by adding responses to symmetrical positive and negative pulses applied to the squid giant axon. I_g was measured in Na^+-free solutions with TTX to block Na^+ channels and internal Cs^+ to block K^+ channels. Since I_g is small, 50 traces had to be averaged in the recording computer to reduce the noise. I_{Na} is measured in normal artificial sea water without TTX. (A) Depolarization from rest elicits an outward "on" I_g that precedes opening of Na^+ channels. (B) Repolarization elicits an inward "off" I_g coinciding with closing of channels (a different axon). (From Hille 1992, adapted from Armstrong and Bezanilla 1974 by copyright permission of the Rockefeller University Press.)

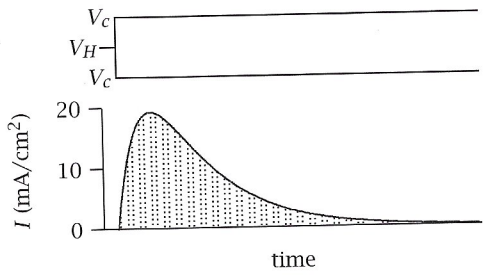

Figure 6.23 Integral of the gating current (shaded area) gives the net gating charge transfer during the voltage step.

Gating current is not blocked by TTX, which blocks I_{Na}. Both I_g and I_{Na} are blocked by $ZnCl_2$, predepolarization, or glutaraldehyde.

The net charge transfer in gating during a single voltage clamp step is given by $Q = zeD$, where z = number of charges on one gating particle, e = elementary electric charge, and D = density of gates ($1/\mu m^2$).

The integral of the time course of the gating current (shaded area, figure 6.23) gives the net charge transformed during a single voltage-clamp step. Experimental results showed $Q = 1882e/\mu m^2$. Kinetic and pharmacological studies attribute almost all mobile gating charges in axons to gating of Na^+ channels. From earlier analysis, 6 charges were thought to be required to open 1 Na^+ gate. Therefore,

$$D = Q/ze = \frac{1882e/\mu m^2}{6e} = 314 \text{ gates}/\mu m^2.$$

Experimentally, Hodgkin and Huxley estimated that $g_{Na} = 1200$ pS/μm^2. Thus, the single-channel conductance for Na^+ channels

$$\gamma = \frac{\overline{g}_{Na}}{D} = \frac{1200 \text{ pS}/\mu m^2}{314 \text{ gates}/\mu m^2} = 3.82 \text{ pS}.$$

The Na^+ gating current shown on the previous page was obtained with short voltage pulses (~ 0.75 msec), which do not elicit much inactivation of the Na^+ channels. Therefore, the total charge transfer at the offset (B, time integral of the inward gating current) is approximately equal to that at the onset, that is, $Q_{on} = Q_{off}$, showing that activation is quick and reversible.

For longer voltage-clamp pulses, the total charge transfer at the offset is less than that at the onset (figure 6.24). After a 10 msec voltage pulse, Q_{off} may be only 30% of Q_{on}, showing that 70% of the gating particles are

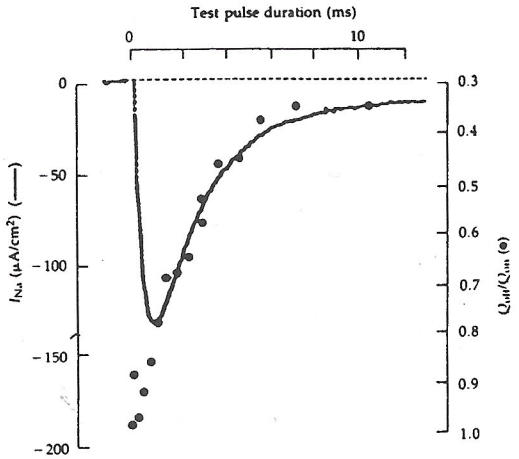

Figure 6.24 Comparison of the time course of inactivation of I_{Na} (solid line) with the immobilization of gating charge (circles) in the squid axon. Gating-charge movement is determined by integrating the rapid "on" and "off" I_g for test pulses of different durations. The fraction of charge returning quickly at the "off" step decreases with increasing pulse length (but not offset of right scale) in parallel with inactivation of Na^+ channels. (From Hille 1992, adapted from Armstrong and Bezanilla 1977 by copyright permission of the Rockefeller University Press.)

immobilized. Immobilization occurs with the same time course as Na^+ channel inactivation (see figure 6.24).

The gating current of K^+ channels is much more difficult to detect than the gating current of Na^+ channels. This is because of the lower density of K^+ channels and their slower activation. Gilly and Armstrong (1980) discovered a prominent slow phase of the gating current that is insensitive to the local anesthetic dibucaine (which reduces Na^+ gating current) in the squid axon. White and Bezanilla (1985) found that the maximum charge transfer associated with the K^+ gating current is about $490e/\mu m^2$ (figure 6.25), and according to the Hodgkin and Huxley measurement of g_K (figure 6.20B), $g_K \propto e^{V/5(\mathrm{mV})}$. Similar to equation 6.6.19, $g_K = \overline{g}_K e^{zV/25(\mathrm{mV})}$ and $z = 5$; therefore 5 charges must be moved to open one K^+ channel.

K^+ channel density, D, can be estimated by

$$D = \frac{Q}{ze} = \frac{490e/\mu m^2}{5e} = 98 \text{ channels}/\mu m^2.$$

This is a high estimate of D: others assume that z for K^+ channel gating is 7–13 e, which makes $D = 36 - 70$ channels/μm^2.

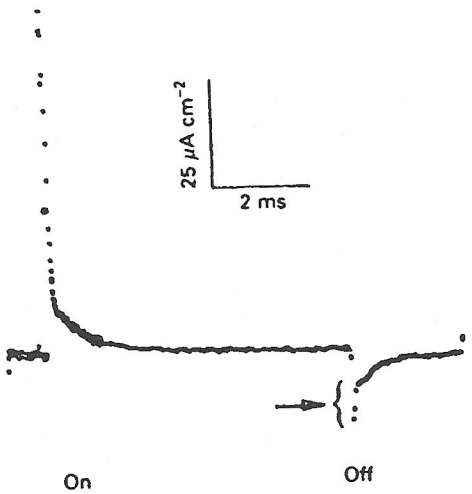

Figure 6.25 K^+ gating current in a perfused squid axon. The internal solution contained impermeant organic cations to eliminate the K^+ ionic current, and the external solution contained Tris nitrate, TTX, and dibucaine to eliminate the Na^+ ionic current and reduce the Na^+ gating current. The gating currents were produced by a 6 msec depolarization from −110 to 0 mV, followed by a return to −60 mV. The "on" response consists of a very brief Na^+ gating current followed by a more slowly changing K^+ gating current. In the "off" response these two components are even more distinct, and the Na^+ gating current (arrow) is smaller. (From Aidley 1989, adapted from White and Bezanilla 1985 by copyright permission of the Rockefeller University Press.)

It is difficult to study the kinetics and charge mobilization of K^+ gating current in the squid axon because it is often masked by the Na^+ gating current (figure 6.25). This problem was overcome recently by studying the gating current of the *Shaker* K^+ channel expressed in *Xenopus* oocytes, which do not contain voltage-gated Na^+ channels (Bezanilla et al. 1991). Figure 6.26 shows the gating currents recorded in normal *Shaker* K^+ channels that exhibit inactivation (A) and mutant *Shaker* K^+ channels that do not exhibit inactivation (B). The gating charge transfer (time integral of the gating current) at the voltage step offset (Q_{off}) for the normal *Shaker* K^+ channel (A) is much less than the gating charge transfer at the voltage step onset (Q_{on}). For the mutant channels in which inactivation is removed (B, similar to the K^+ channels in the squid axon), $Q_{off} = Q_{on}$ although the time course of the gating current at the voltage offset is slower than that at the voltage onset.

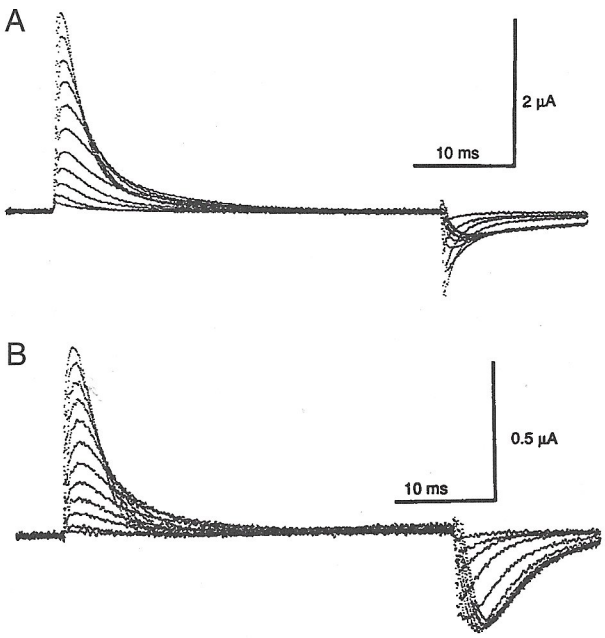

Figure 6.26 Gating currents recorded from normal *Shaker* K^+ channels (A) and from the non-inactivating mutant *Shaker* K^+ channels (B) expressed in *Xenopus* oocytes. The gating currents were activated by depolarizing voltage-clamp steps ranging from −70 mV to 30 mV in 10 mV steps. (From Bezanilla et al. 1991. Used by permission of AAAS, copyright © 1991 AAAS.)

Example 6.1

The Na^+ ionic current I_{Na} and Na^+ gating current I_g in the squid axon produced by a depolarizing voltage step (from −70 mV to +20 mV) under voltage clamp are shown in the figure below. The lower trace shows currents recorded in an artificial sea water with only one fifth of the normal Na^+ concentration, for depolarizations from −70 mV to +20 mV. The initial brief outward current is gating current, followed by the much larger inward Na^+ ionic current. The upper trace shows the gating currents alone, after blocking the Na^+ ionic currents with TTX and eliminating capacitive currents. K^+ currents were eliminated by using K^+-free solutions for both internal and external media.

Example 6.1 (continued)

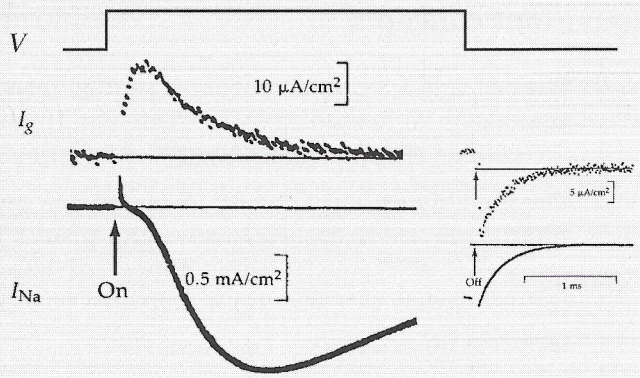

a. Explain why I_g is outward at the pulse onset and inward at the pulse offset. Why is the amplitude of the I_g at the offset smaller than that at the onset?

b. Why is there a transient inward I_{Na} at the offset of the voltage pulse?

c. Under what condition do you expect to observe symmetrical I_g at the onset and offset of the voltage pulse?

Answer to example 6.1

a. I_g is outward at pulse onset because the depolarization results in an increase of an outward electric field, which pushes the gating particles outward. At pulse offset, the electric field changes in the opposite direction, and thus I_g is inward. I_g is smaller at the offset because a substantial fraction of Na^+ channels is in the inactivated state after the voltage pulse is maintained for about 3.25 msec.

b. The inward transient I_{Na} at offset is caused by the instantaneous voltage drop (from −20 to −70 mV), which results in a much larger driving force ($V - E_{Na}$), and the time-dependent closure of Na^+ channels. (Na^+ channels do not have enough time to close immediately after the pulse offset.)

c. I_g will be symmetrical if the voltage pulses are shorter than 1 msec, which is not long enough for significant inactivation to take place.

6.7 Review of important concepts

1. The Na^+ and K^+ conductances mediating the action potentials in the squid axon were studied by Hodgkin and Huxley (1952a–d) by using the voltage-clamp technique and the gate model.
2. The instantaneous I-V relations of the Na^+ and K^+ channels in the squid axon are linear. Voltage-clamp results suggest that the Na^+ channel is activated by three gating particles (m) and one inactivating particle (h), and the K^+ channel is activated by four gating particles (n).
3. The voltage- and time-dependent parameters of the Na^+ and K^+ conductances were quantitatively described by the Hodgkin and Huxley equations. The simulated action potential based on these equations is in excellent agreement with the recorded action potential. The propagation and conduction velocity of action potentials can also be described by these equations.
4. Mechanisms mediating various dynamic features of action potentials such as threshold, refractory period, and accommodation can be described by changes of I-V relations of the Na^+ and K^+ currents in the cell.
5. The gating currents of the Na^+ and K^+ channels were recorded by eliminating all ionic currents and the capacitive current. From the charge transfer of the gating currents, one can estimate the number of gating particles per charge, channel density, and single-channel conductance in the membrane.